1. INTRODUCTION

On Friday, September 6, 2024, Boeing's Starliner spacecraft undocked from the International Space Station (ISS), with vehicle separation confirmed at GMT 22:04. The unmanned module landed about 6 hours later at the White Sands Space Harbor in New Mexico. As depicted in Figure 1 on page 4, we see the ISS configuration prior to Starliner's departure, the station accommodates various visiting vehicles. In the interest of crew safety, it was determined that the Starliner would undock without its two crew members and return to Earth unmanned.

Visiting vehicles like Boeing's Starliner and others, such as SpaceX's Dragon or the Russian Soyuz, use a spring-based mechanism for their initial separation from the ISS. This provides a passive, reliable method of separation without requiring complex thruster coordination at the moment of undocking. Once the spacecraft is mechanically released from the docking port, a set of spring-loaded mechanisms provides the push needed to initiate separation. These springs are located in the docking mechanism. They push the vehicle away at a relatively slow, controlled rate, ensuring that the spacecraft drifts safely away without damaging the ISS. After the initial separation, the spacecraft relies on its onboard thrusters to perform a series of controlled burns. These burns increase the distance between the spacecraft and the ISS in a well-orchestrated fashion and move it to a safe distance for re-entry or further maneuvers. This document examines the vibratory impact on the space station's microgravity environment resulting from the Boeing Starliner undocking (initial separation) event.

2. QUALIFY

Figure 2 on page 5 shows spectral calculation results from measurements made by the Space Acceleration Measurement System (SAMS) sensor head (S/N 121f08) in the Columbus module (in rack COL1A3) for a ~30-minute span with a tick mark at time of undocking event at GMT 2024-09-06/22:04. Note the structural frequency excitation (red, horizontal streak) at just about 0.19 Hz and lasting several seconds. All SAMS sensors distributed throughout the ISS show a similar structural response to the Starliner undocking event - after effects of the passive spring push.

Similar to the plot in the previous figure, we see other perspectives from two other SAMS sensor heads:

1) Figure 3 on page 6 from a SAMS sensor head in the JEM (JPM1F1).
2) Figure 4 on page 7 from a SAMS sensor head in the LAB (LAB1P2).

3. QUANTIFY

The two, per-axis acceleration versus time plots of Figure 5 on page 8 serve to quantify the vibratory impact of the Starliner undocking event just after GMT 22:04, with both sensors being located in the Columbus module. These 2 plots also show effects apparent for at least a few minutes afterward as the larger appendages of the space station ringout in response to the two massive vehicles being "sprung apart". The SAMS sensors, of course, are on the heavier of the 2 vehicles (the ISS), so we are measuring the impact on the space station. Invoking Newton's nth Law we would expect the less massive vehicle (Starliner) to experience a somewhat larger acceleration.

The two per-axis acceleration versus time plots of Figure 5 on page 8 serve to quantify the vibratory impact of the Starliner undocking event just after GMT 22:04, with both sensors located in the Columbus module. These plots also show effects that remain apparent for at least a few minutes afterward, as the larger appendages of the space station continue to oscillate due to the "springing apart" of the two massive vehicles.

The SAMS sensors, positioned on the heavier vehicle (the ISS), record the vibratory impact on the space station. According to Newton's second law of motion, expressed as:

$$\vec{F} = m\vec{a}$$

where $\vec{F}$ is the force applied, m is the mass of the object, and $\vec{a}$ is its acceleration. Since the spring force exerted on both vehicles is the same, we can relate the masses and accelerations of the two vehicles. The ratio of the masses is equal to the reciprocal of the accelerations:

$$\frac{m_{ISS}}{m_{Starliner}} = \frac{a_{Starliner}}{a_{ISS}}$$

Even though we did not directly measure it, we know that the less massive vehicle (Starliner) experienced a greater acceleration compared to the ISS when acted upon by the same spring force according to Newton's second law.

Similar to the plot in the previous figure, we see other perspectives from other SAMS sensor heads:

1) Figure 6 on page 9 for 2 SAMS sensor heads in the LAB.
2) Figure 7 on page 10 for 1 SAMS sensor head in the JEM.

Acceleration Vector Directionality

Referring back to Figure 1, in particular the location of Starliner before undocking and the +X-direction indicated by the cyan arrow, it should be evident that a spring force acting between Starliner and the much more massive ISS would provide Starliner with an acceleration in the +X-direction and, by Newton's third law of action/reaction, a smaller acceleration in the -X-direction experienced on the space station. Focusing on the time just before the 70-second mark in a zoom-in on time for SAMS measurements plotted in the following figures reinforce our directionality assertion here:

1) Figure 8 on page 11 for 2 SAMS sensor heads in the COL.
2) Figure 9 on page 12 for 2 SAMS sensor heads in the LAB.
3) Figure 10 on page 13 for 1 SAMS sensor head in the JEM.

In these plots, we see primarily the -X-direction acceleration from the springs push just before the 70-second mark followed by at least some ringout from the structural response. Most notably, we see structural ringout in the Columbus module SAMS data.

Acceleration Vector Magnitude

For comparison, we also plotted acceleration vector magnitude versus time in the following figures:

1) Figure 11 on page 14 for 4 SAMS sensor heads in the COL & LAB.
2) Figure 12 on page 15 for 1 SAMS sensor head in the JEM.

where we note the largest acceleration vector magnitude excursions in the LAB1P2 and COL1A3 SAMS sensor head locations. As a result, we took a look at the 200 Hz data from these 2 sensor heads as shown in Figure 13 on page 16. These do show some signs of the undocking event just before the 70-second mark, but less distinctly than the lower frequency (6 Hz) data we presented earlier.

As a side note based on the pattern observed in the Z-axis data for the 121f04 sensor head, we also plotted the per-axis power spectral densities for these same 2 sensor heads to see that the Z-axis pattern seen in the time domain data comes from some combination of the 2 spectral peaks near 55 Hz, which we show in a different document is equipment associated with the Cold Atom Lab in the LAB1P2 rack.

See this document for more on this aside regarding Cold Atom Lab equipment.

4. CONCLUSION

The undocking of Boeing's Starliner spacecraft from the ISS on September 6, 2024, marked a significant milestone in that an unplanned unmanned mission was initiated. The mission's successful conclusion, with the vehicle safely landing at White Sands Space Harbor, demonstrated the robustness of the ISS program to handle unforeseen vehicle anomalies.

Vibratory analysis conducted for the undocking event provided empirical acceleration data on the space station's structural response under these dynamic conditions.

The ultimate findings from Boeing Starliner's extended stay at the ISS underscore the importance of ongoing testing and evaluation of visiting vehicles, ensuring that safety standards are maintained at the highest level, especially for crewed operations.

TABLE 1. Table of Figures

Figure	Page	Type	Frequency	Time Span	Comment
1	4	Graphic	n/a	n/a	ISS Graphic Shows Starliner Docked at Node 2 Forward Port
2	5	SpG	< 6 Hz	~30 min.	Undocking at ~GMT 22:04, SAMS in COL
3	6	SpG	< 6 Hz	~30 min.	Undocking at ~GMT 22:04, SAMS in JEM
4	7	SpG	< 6 Hz	~30 min.	Undocking at ~GMT 22:04, SAMS in LAB
5	8	GvT	< 6 Hz	4 min.	Undocking at ~GMT 22:04, SAMS in COL
6	9	GvT	< 6 Hz	4 min.	Undocking at ~GMT 22:04, SAMS in LAB
7	10	GvT	< 6 Hz	4 min.	Undocking at ~GMT 22:04, SAMS in JEM
8	11	GvT Zoom	< 6 Hz	45 sec.	Undocking Just Before 70-sec. Mark, SAMS in COL
9	12	GvT Zoom	< 6 Hz	45 sec.	Undocking Just Before 70-sec. Mark, SAMS in LAB
10	13	GvT Zoom	< 6 Hz	45 sec.	Undocking Just Before 70-sec. Mark, SAMS in JEM
11	14	Mag	< 6 Hz	45 sec.	Undocking Just Before 70-sec. Mark, SAMS in COL & LAB
12	15	Mag	< 6 Hz	45 sec.	Undocking Just Before 70-sec. Mark, SAMS in JEM
13	16	GvT	< 200 Hz	45 sec.	Undocking Just Before 70-sec. Mark, SAMS in LAB & COL
14	17	PSDs	40-90 Hz	4 min.	Starting at 22:03:00, SAMS in LAB & COL

SpG: Spectrogram
GvT: Per-Axis Acceleration versus Time
GvT Zoom: Zoom-In of Per-Axis Acceleration versus Time
Magnitude: Acceleration Vector Magnitude versus Time
PSDs: Per-Axis Power Spectral Densities

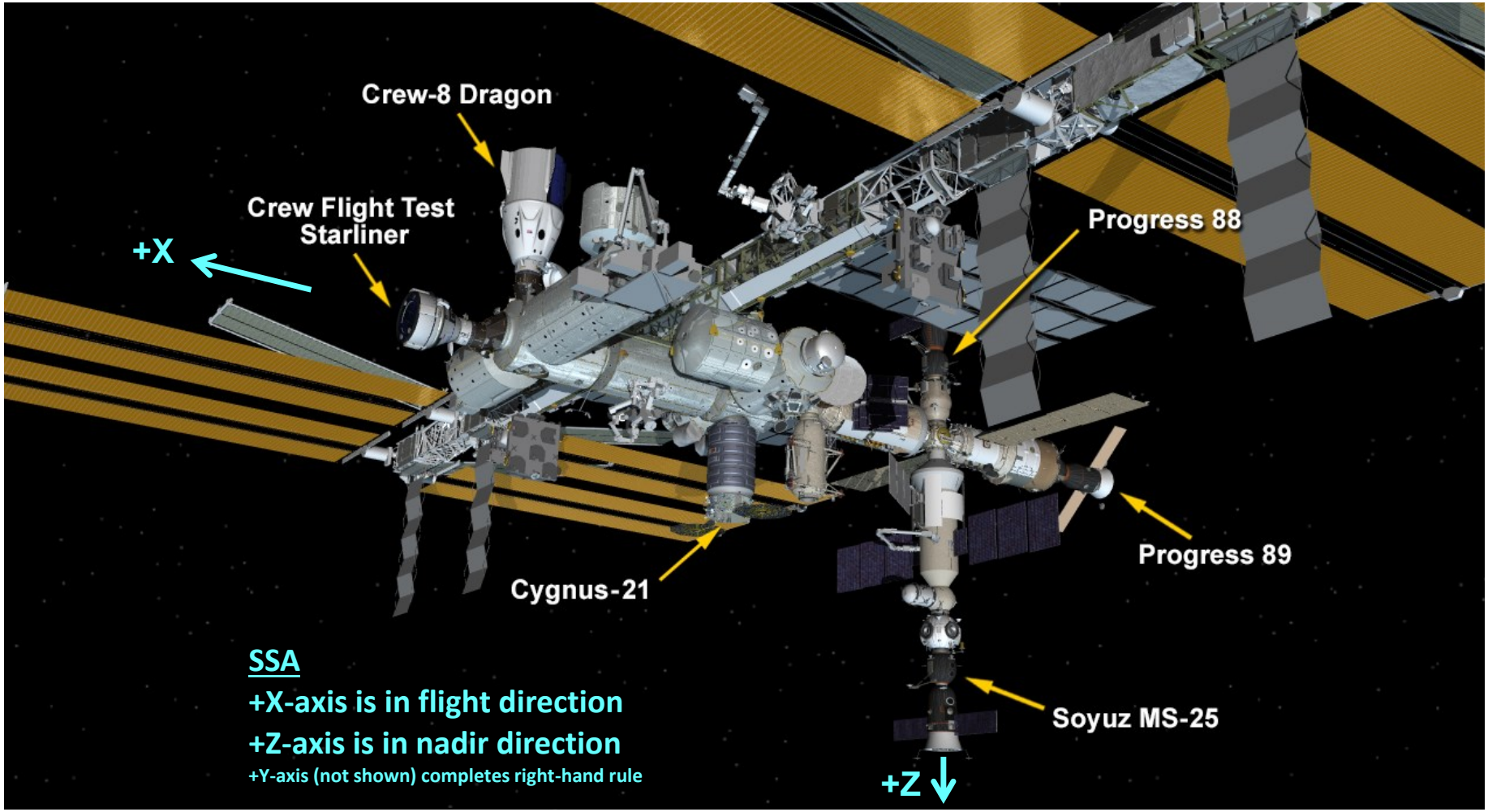

Fig. 1: ISS Visiting Vehicle Configuration Before Boeing Starliner Undocking on GMT 2024-09-06.

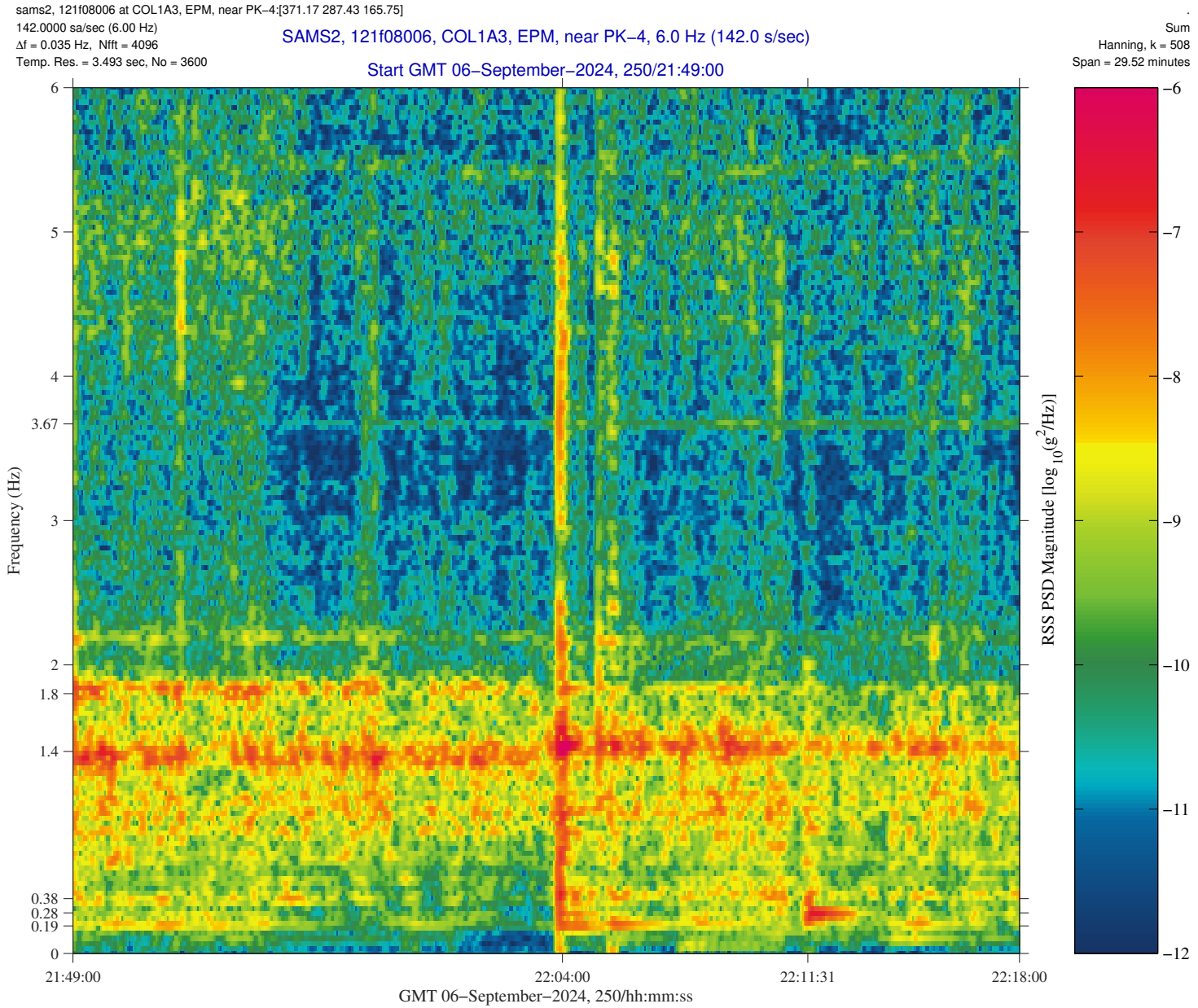

Fig. 2: SAMS Sensor 121f08 in COL, Below 6 Hz, ~30-Minute Spectrogram Starting at GMT 2024-09-06/21:49.

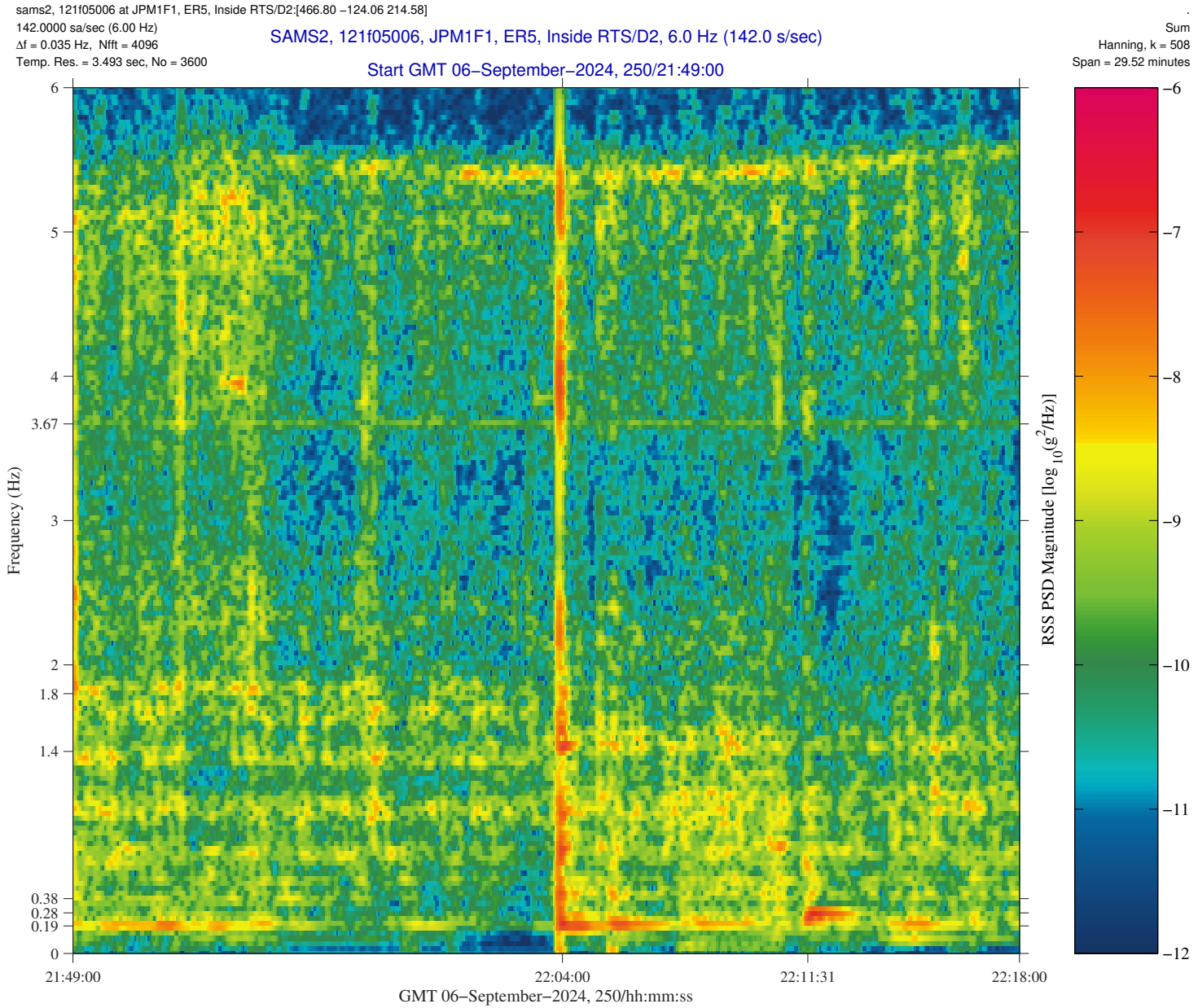

Fig. 3: SAMS Sensor 121f05 in JEM, Below 6 Hz, ~30-Minute Spectrogram Starting at GMT 2024-09-06/21:49.

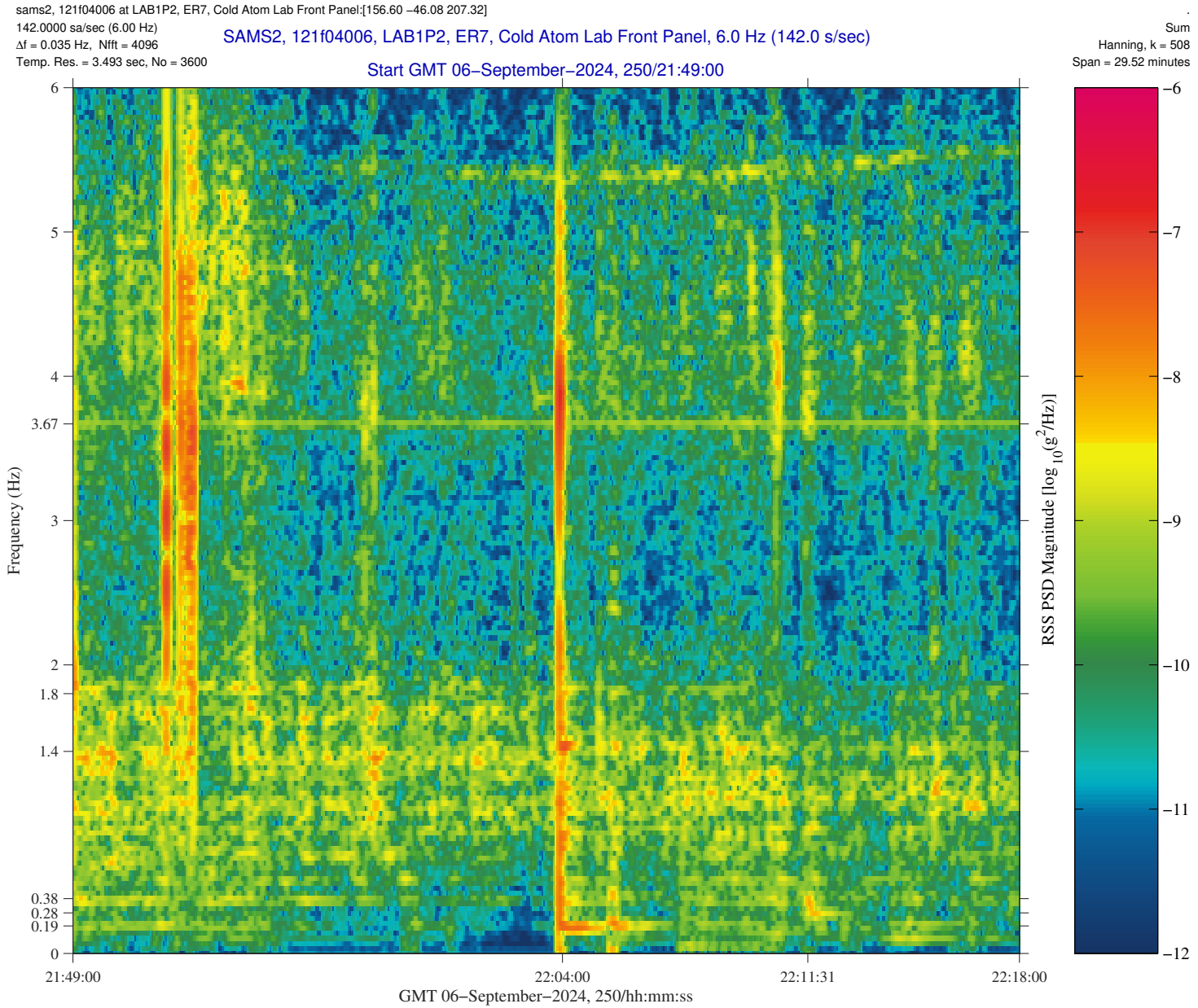

Fig. 4: SAMS Sensor 121f04 in LAB, Below 6 Hz, ~30-Minute Spectrogram Starting at GMT 2024-09-06/21:49.

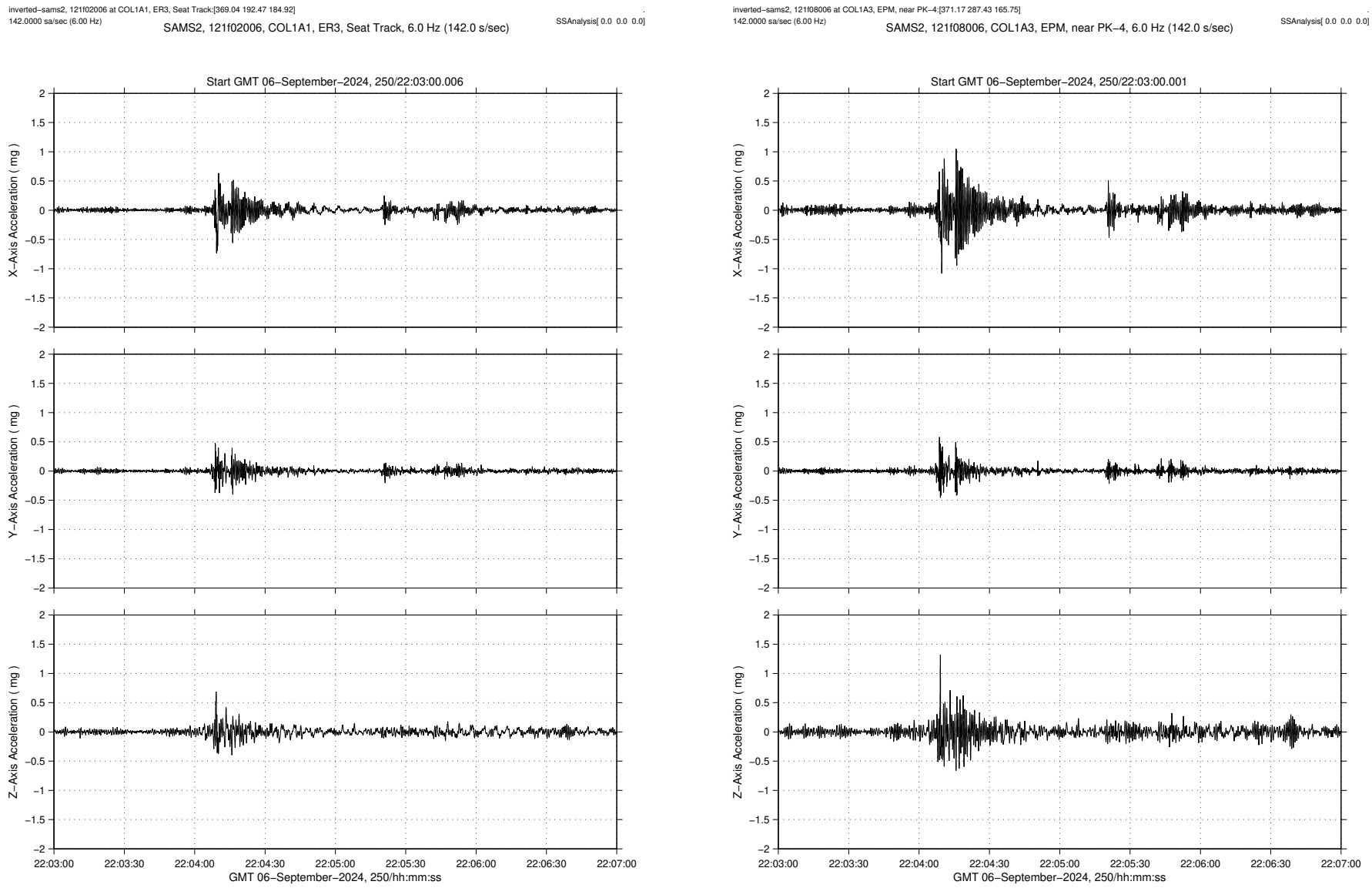

Fig. 5: SAMS in COL Below 6 Hz, 4-Minute Per-Axis Accel. vs. Time Starting at GMT 2024-09-06/22:03:00 (left) **121f02 at COL1A1**, (right) **121f08 at COL1A3**.

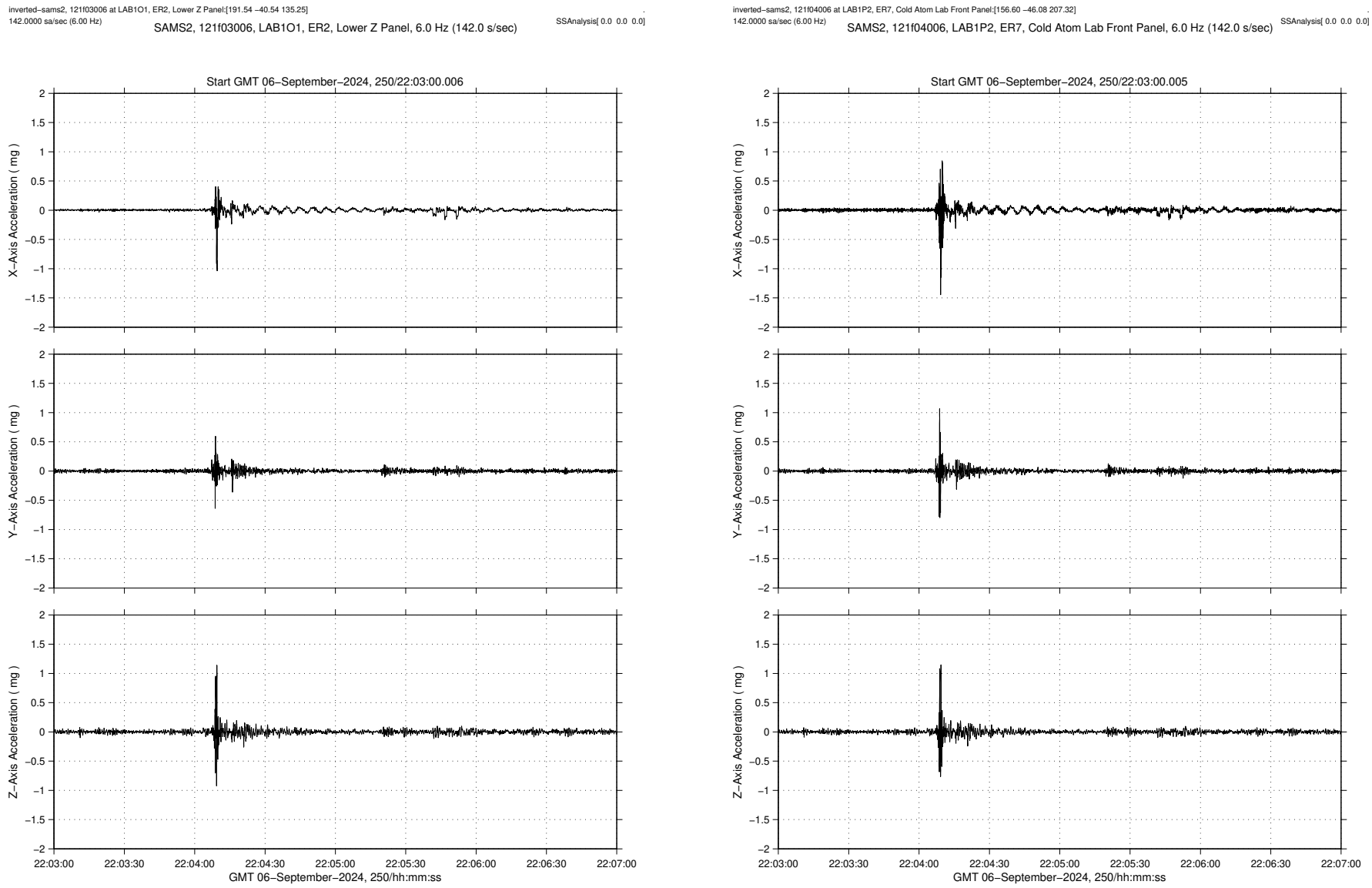

Fig. 6: SAMS in LAB Below 6 Hz, 4-Minute Per-Axis Accel. vs. Time Starting at GMT 2024-09-06/22:03:00 (left) **121f03 at LAB1O1**, (right) **121f04 at LAB1P2**.

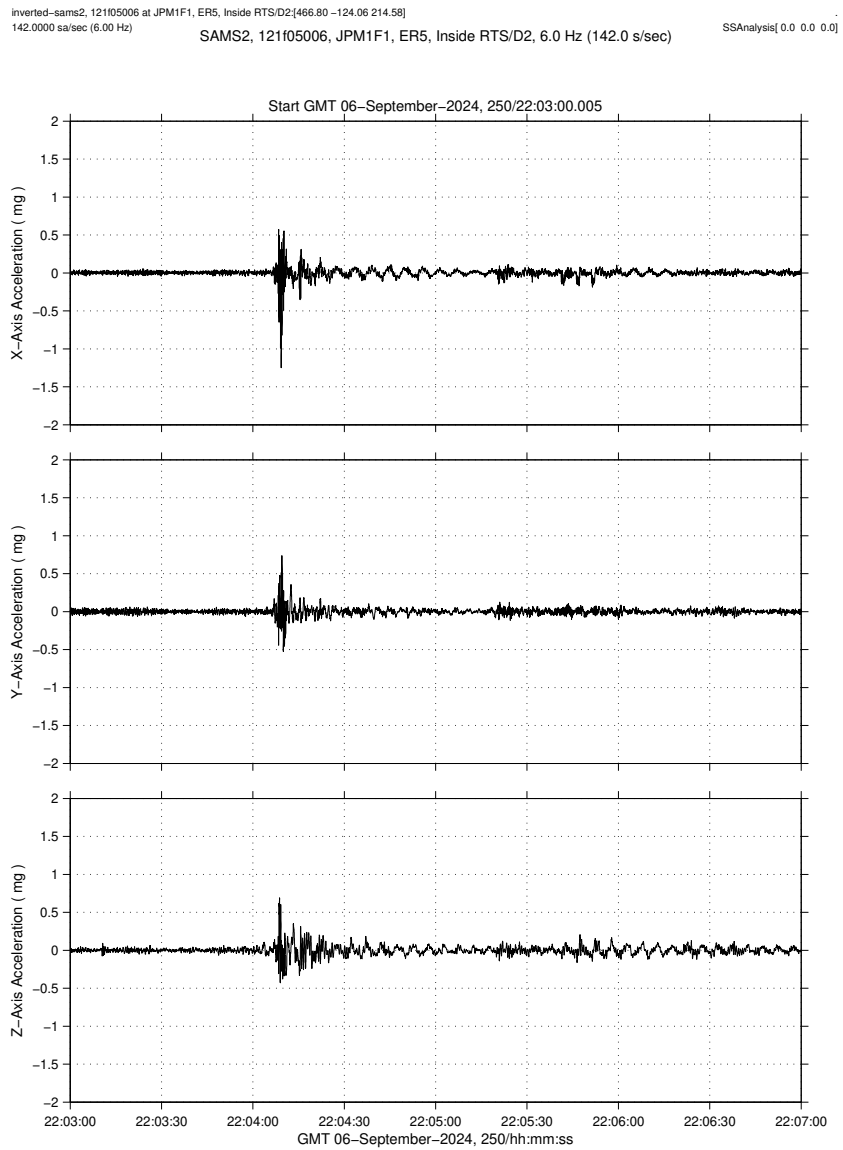

Fig. 7: SAMS in JEM Below 6 Hz, 4-Minute Per-Axis Accel. vs. Time Starting at GMT 2024-09-06/22:03:00 (left) **121f05 at JPM1F1**.

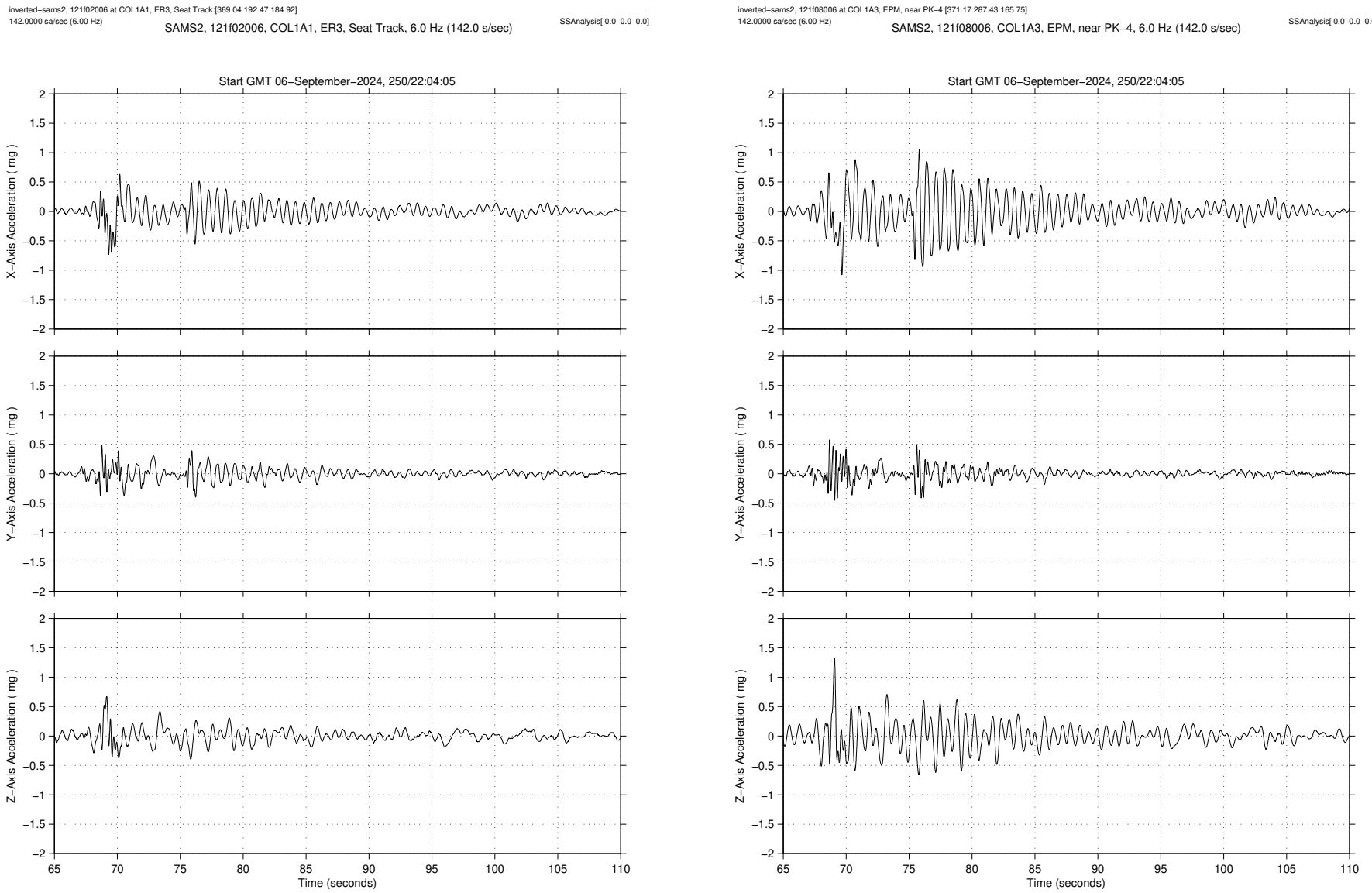

Fig. 8: SAMS in COL Below 6 Hz, 45-Second Per-Axis Accel. vs. Time Starting at GMT 2024-09-06/22:04:05 (left) **121f02 at COL1A1**, (right) **121f08 at COL1A3**.

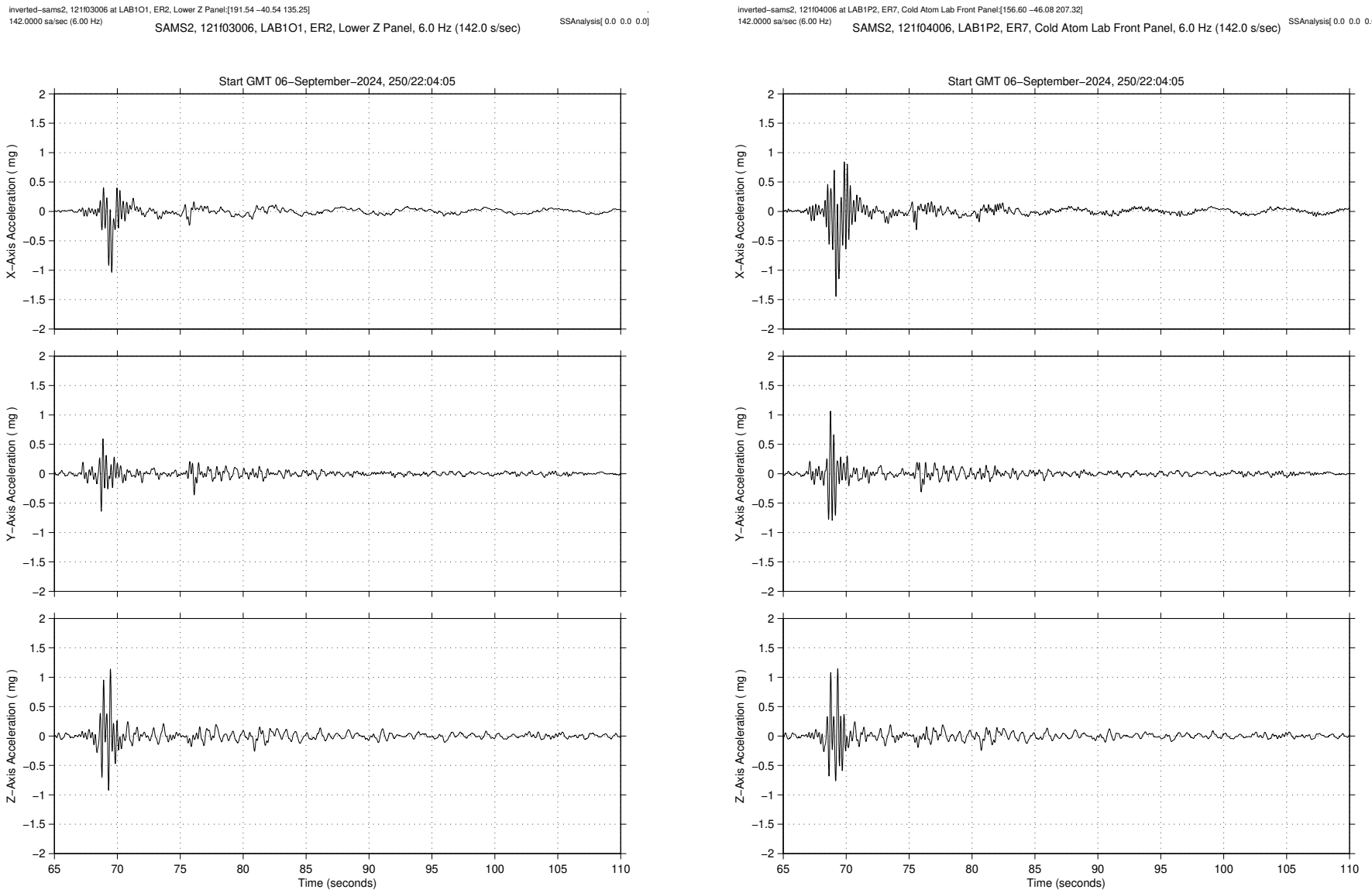

Fig. 9: SAMS in LAB Below 6 Hz, 45-Second Per-Axis Accel. vs. Time Starting at GMT 2024-09-06/22:04:05 (left) **121f03 at LAB1O1**, (right) **121f04 at LAB1P2**.

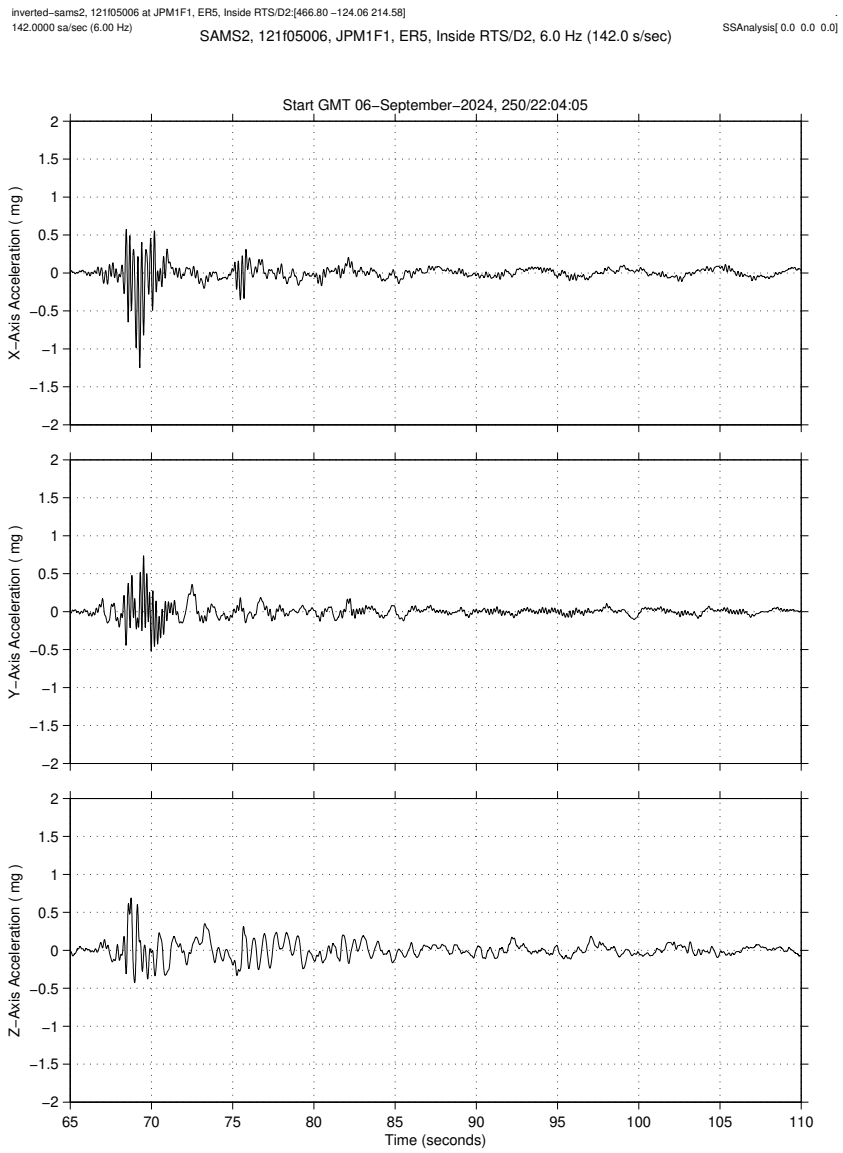

Fig. 10: SAMS in JEM Below 6 Hz, 45-Second Per-Axis Accel. vs. Time Starting at GMT 2024-09-06/22:04:05 (left) **121f05 at JPM1F1**.

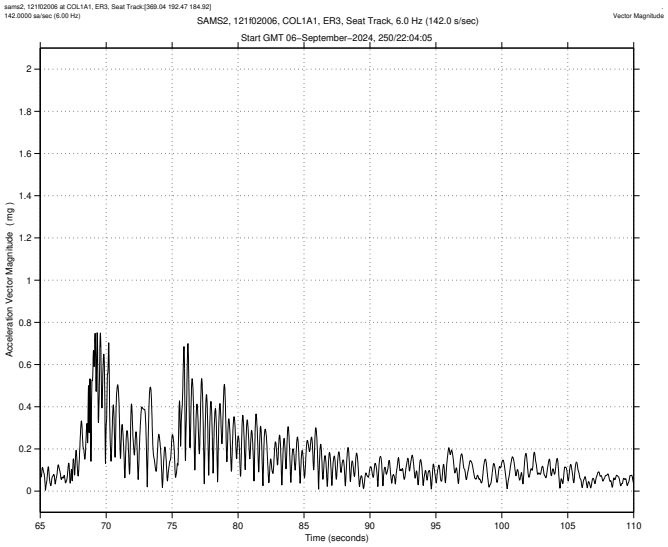

(a) 121f02 at COL1A1

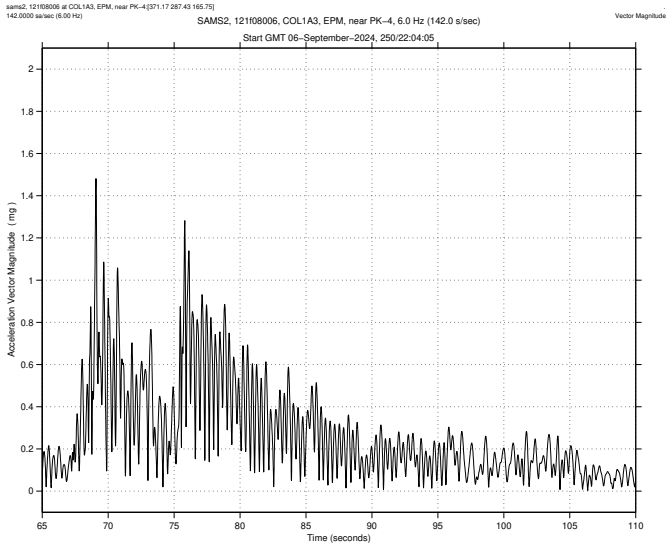

(b) 121f08 at COL1A3

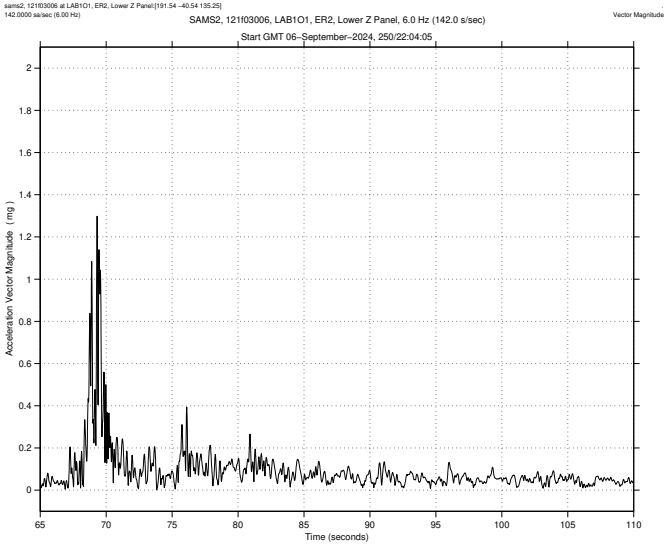

(c) 121f03 at LAB1O1

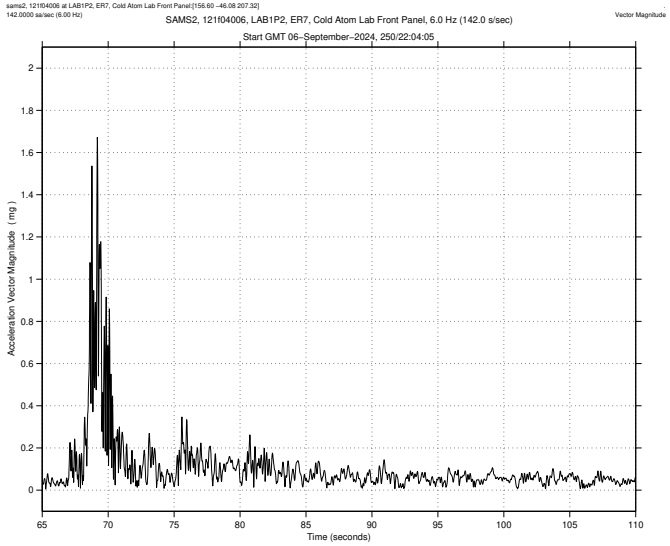

(d) 121f04 at LAB1P2

Fig. 11: SAMS Below 6 Hz, 45-Second Acceleration Magnitude vs. Time Starting at GMT 2024-09-06/22:04:05

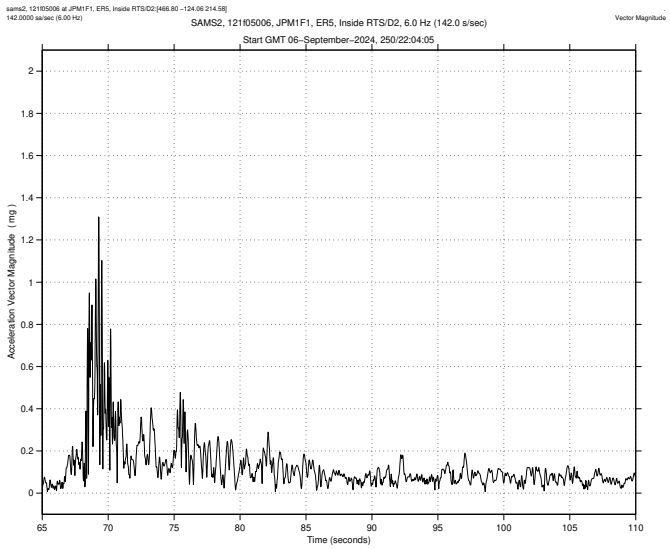

121f05 at JPM1F1

Fig. 12: SAMS Below 6 Hz, 45-Second Acceleration Magnitude vs. Time Starting at GMT 2024-09-06/22:04:05

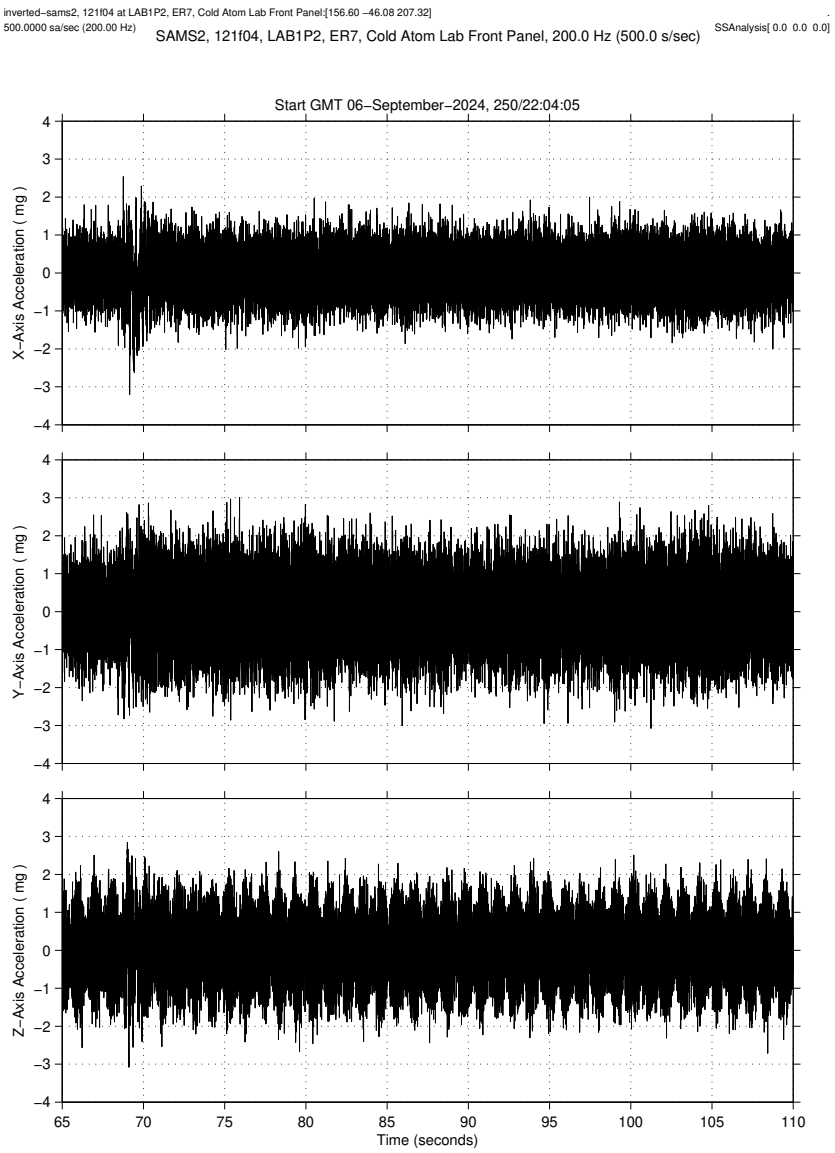

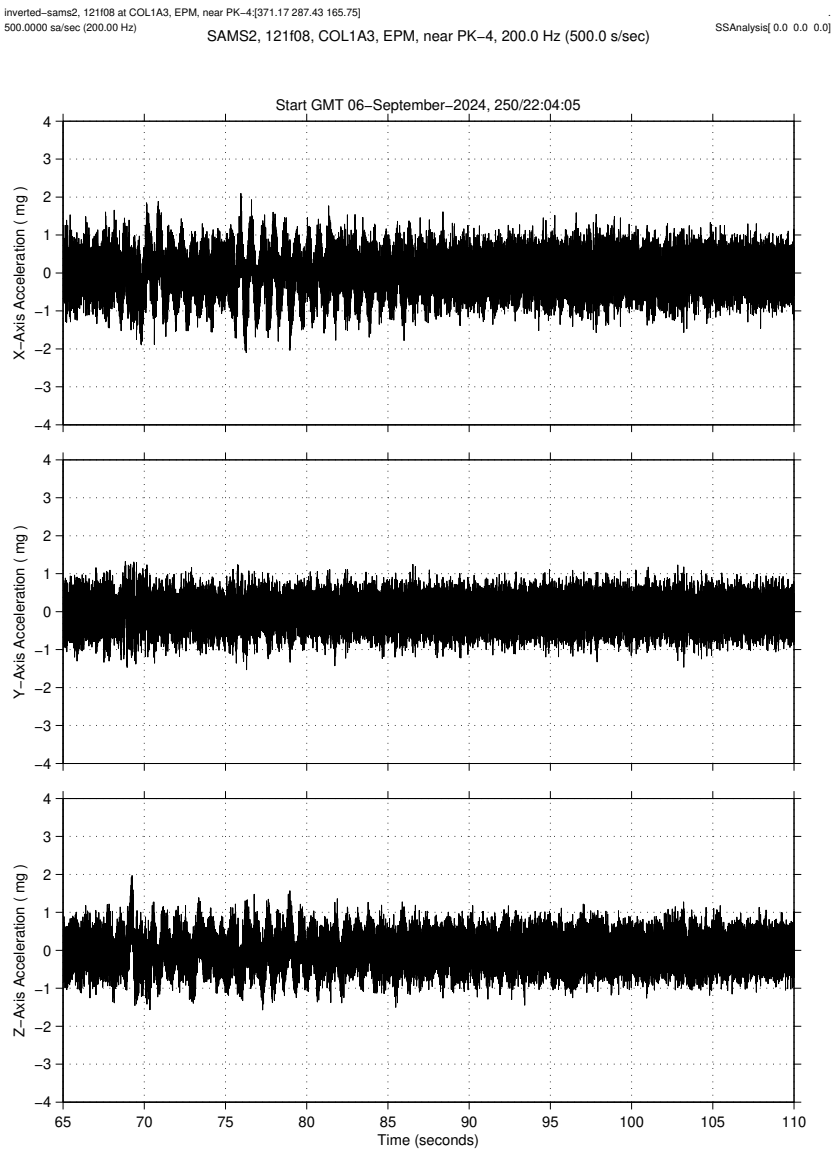

Fig. 13: SAMS Up to 200 Hz, 45-Second Per-Axis Accel. vs. Time Starting at GMT 2024-09-06/22:04:05 (left) **121f04 at LAB1P2**, (right) **121f08 at COL1A3**.

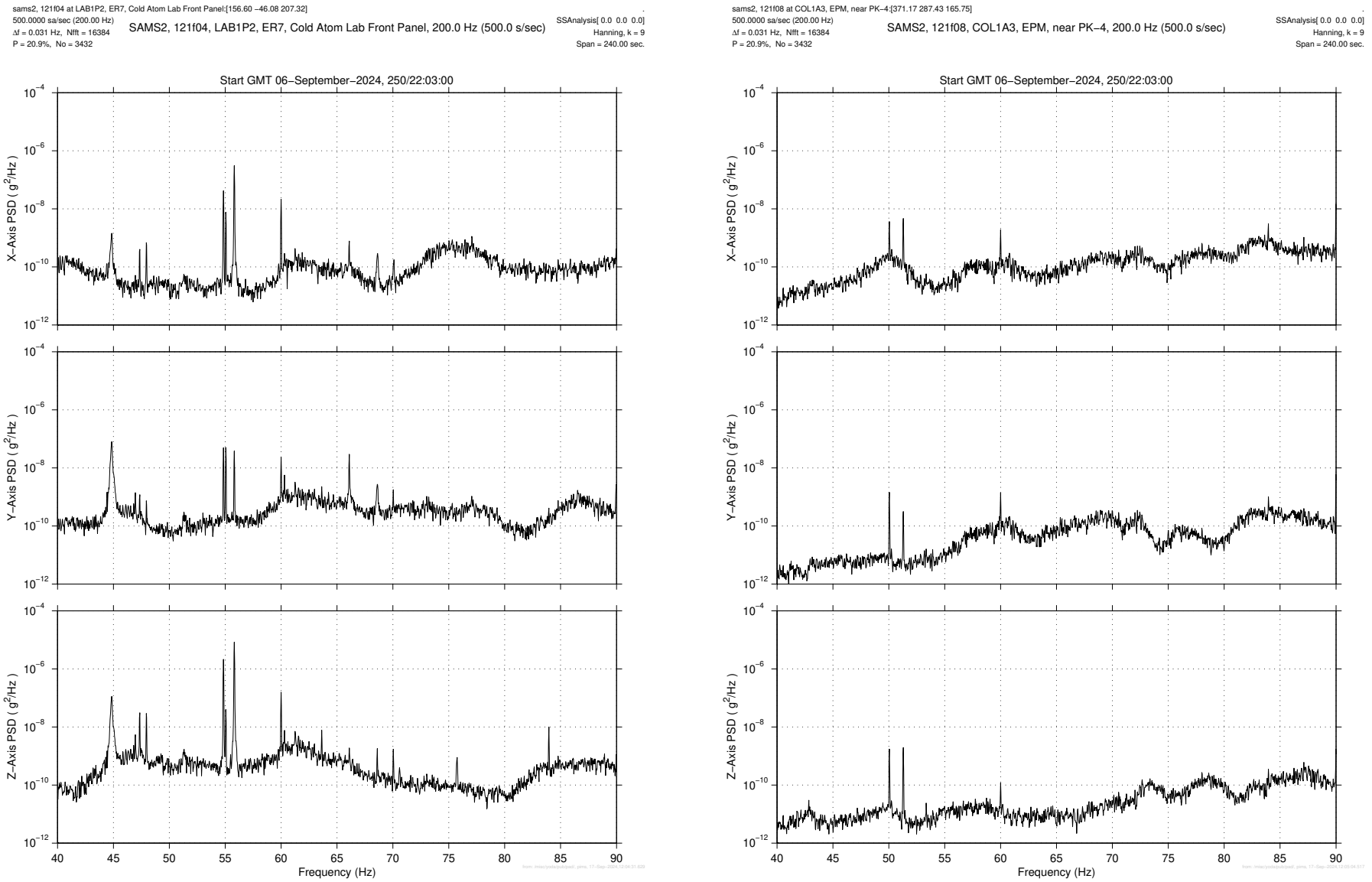

Fig. 14: SAMS 40-90 Hz, 4-Minute PSDs Starting at GMT 2024-09-06/22:03:00 (left) **121f04 at LAB1P2**, (right) **121f08 at COL1A3**.